MODELING OF TIRE–SOIL INTERACTION: THE INFLUENCE OF INFLATION PRESSURE AND PERMISSIBLE LOADS ON CONTACT PATCH AREA

Serhii Sokolik[1][0000-0001-4496-8681], Andrii Kozhushko[2][0000-0002-4725-5911], Vladyslav Zubko[1][0000-0002-2426-2772], Mykhailo Shuliak[1][0000-0001-7286-6602], Oleksandr Yaryta[3][0000-0003-4948-6577]
[1]*Sumy National Agrarian University, Kharkiv, Ukraine*
[2]*National Technical University "Kharkiv Polytechnic Institute", Kharkiv, Ukraine*
[3]*Kharkiv National Automobile and Highway University, Kharkiv, Ukraine*
E-mails: s.sokolik@snau.edu.ua

Abstract - The interaction between agricultural tires and soil plays a crucial role in determining traction performance, energy efficiency, and soil compaction. One of the key parameters governing this interaction is the contact patch area, which depends on tire design, inflation pressure, and applied load. However, many existing analytical models rely on simplified assumptions regarding contact geometry, which limits their accuracy under real operating conditions. The aim of this study is to develop and analyze a mathematical model of tire–soil interaction that accounts for the influence of inflation pressure and permissible loads on the contact patch area. The proposed approach systematizes the calculation procedure by combining the classical method for determining contact length and width based on the Lyasko model with an improved representation of the contact patch geometry using a superellipse formulation. This allows for a more realistic description of the tire–soil interface. The model was applied to analyze tire systems of Trelleborg and Mitas brands used on the Case IH Magnum 400 tractor. The input parameters, including tire dimensions, permissible loads, and inflation pressure ranges, were identified and used to evaluate the variation of the contact patch area. The results show that the contact area increases with load and decreases with inflation pressure, although the relationship is nonlinear. It was established that the Mitas 600/70 R30 tire provides an 8–52.3% larger contact area compared to the Trelleborg 600/70 R30 tire. For rear tires, the Trelleborg 710/75 R42 exhibits a 13.5% larger contact area at minimum pressure, while at maximum pressure the Mitas 710/70 R42 provides a 44.3% larger contact area. The obtained results are consistent with experimental data reported in the literature, while the use of a superellipse-based approach improves the accuracy of contact area estimation. The proposed model can be applied for engineering analysis and optimization of tire operating parameters aimed at reducing soil compaction and improving agroecological performance.

Keywords: Wheeled tractor, Tire–soil interaction, Contact patch area, Superellipse model, Permissible loads, Inflation pressure, modeling.

1. Introduction

The interaction between agricultural tires and soil plays a crucial role in determining the operational efficiency, energy consumption, and environmental impact of modern farming systems. The tire–soil interface represents the final stage of power transmission from the tractor to the ground, where significant energy losses occur due to soil deformation and slippage. It is estimated that traction efficiency in agricultural conditions may be as low as 60%, highlighting the importance of optimizing tire parameters and operating conditions [1]. A crucial aspect of tire–soil interaction is its direct influence on traction performance and overall efficiency of tractor–implement systems. Recent studies have shown that achieving maximum traction efficiency requires not only optimization of traction force but also a rational distribution of mass and vertical reactions between tractor wheels [2, 3]. In particular, it has been demonstrated that the distribution of vertical loads and coupling weight

dx.doi.org/10.17683/ijomam/issue24.34

significantly affects traction properties and operational efficiency, especially under variable field conditions [2, 3].

One of the key factors influencing tire–soil interaction is the distribution of vertical stress beneath the wheel, which directly affects soil compaction, rut formation, and crop productivity. Excessive stress levels can lead to deterioration of soil structure, reduced porosity, and decreased water infiltration, ultimately impacting plant growth and yield [4].

Classical terramechanics theories, particularly those developed by Bekker and Wong, provide a fundamental framework for describing soil deformation under wheel loads. These approaches are widely used in analytical and semi-empirical models, where the pressure–sinkage relationship and shear stress behavior are key components [5]. However, many existing models rely on simplified assumptions regarding the geometry of the tire–soil contact patch, often approximating it as a circular or elliptical shape.

Recent studies have shown that the actual geometry of the contact patch is significantly more complex and depends on tire deformation, soil properties, inflation pressure, and applied load. Advanced modeling approaches, including numerical simulations (FEM and DEM), have been developed to better capture these effects, but they require high computational resources and are not always suitable for practical engineering applications [1].

Therefore, there is a need for improved analytical models that provide a more accurate representation of the contact patch geometry while maintaining computational efficiency. In particular, the use of superellipse-based formulations offers a promising approach for refining contact area estimation and improving the prediction of stress distribution.

The aim of this study is to develop a mathematical model of tire–soil interaction that accounts for the influence of inflation pressure and permissible loads on the contact patch area. The proposed approach integrates analytical modeling with experimentally validated parameters and provides a basis for improving agroecological performance and reducing soil compaction in agricultural systems.

2. Literature Review

The study of tire–soil interaction has evolved from classical empirical models toward more advanced analytical and experimental approaches. Early work by Bekker and subsequent developments in terramechanics established the fundamental relationships describing soil deformation under loading conditions. These models remain widely used; however, their accuracy strongly depends on the correct estimation of the tire–soil contact area.

Modern research in tire–soil interaction can be broadly classified into three categories: experimental studies, analytical (semi-empirical) modeling, and numerical simulations. Experimental approaches provide direct measurements of contact area, stress distribution, and soil deformation. For example, recent studies using 3D scanning techniques have demonstrated that both inflation pressure and vertical load significantly influence the size and shape of the tire contact patch [6].

Analytical models aim to balance accuracy and computational efficiency. Many of these models still assume simplified contact geometries, such as circular or elliptical shapes, which can lead to inaccuracies in predicting stress distribution. Recent works have proposed improvements by modifying contact area formulations and incorporating tire deformation effects. For instance, in the work [1] autors introduced an improved traction model that accounts for variations in the contact patch geometry and demonstrated strong correlation with experimental data.

One of the key challenges in modeling tire–soil interaction is the accurate representation of the contact patch geometry. Traditional approaches often assume circular or elliptical shapes, which simplify calculations but introduce significant deviations from real conditions. Experimental investigations have shown that the actual contact area depends on multiple factors, including tire construction, inflation pressure, vertical load, and soil properties.

A significant contribution to improving contact area modeling was presented by Marušiak et al., who verified several analytical models using experimental data obtained from tractor–trailer unit testing [7]. Their results demonstrated that the superellipse-based approach provides the highest agreement with measured data, achieving up to 81% accuracy when using measured half-axes and up to 95% for trailer tires. Although some empirical models also showed comparable accuracy, the superellipse method was identified as more physically consistent due to its ability to represent the actual geometry of the tire–soil interface.

Experimental studies further confirm the strong influence of operational parameters on the contact area. For example, Schwanghart reported that the contact area increases with increasing wheel load and decreasing inflation pressure [8]. However, the relationship is nonlinear: doubling the load results in only a 30–40% increase in contact area, while doubling the inflation pressure reduces the contact area to approximately 70–80% of its original value. These findings highlight the complexity of tire–soil

interaction and the limitations of simplified linear models.

More recent experimental research by Alkhalifa et al. provided detailed insights into the effects of vertical load and inflation pressure on tire–soil interaction using instrumented soil bin tests [9]. Their results showed that reducing inflation pressure significantly increases contact length (up to 39%), while vertical load has a statistically significant effect on contact dimensions. Interestingly, the measured contact area on deformable soil was found to be up to 3.3 times greater than on rigid surfaces, emphasizing the importance of accounting for soil deformation in analytical models.

Modern research integrates these experimental findings into analytical and numerical models. While FEM and DEM approaches allow detailed simulation of soil behavior, they remain computationally expensive. Therefore, there is a growing interest in improving analytical models by incorporating more realistic geometric representations of the contact patch.

Despite these advancements, many existing models still rely on simplified assumptions regarding contact geometry. This creates a gap between theoretical predictions and experimental observations. The use of superellipse-based formulations offers a promising solution to this problem by providing a flexible and physically meaningful representation of the contact area.

3. Materials and Methods

3.1. Vertical Stress Beneath the Center of a Wheel

The development of a mathematical model of the The determination of vertical stress beneath the center of a wheel is an important stage in the analysis of the interaction between a machine–tractor unit and the supporting surface. Vertical stress defines the intensity of load transfer from the wheel to the soil and directly affects the load-bearing capacity of the soil layer, rut depth, and the degree of soil compaction.

During the operation of a machine–tractor unit, the vertical component of the load is concentrated within the tire–soil contact zone, with maximum stress values observed near the center of the tire footprint. The stress distribution depends on a number of factors, including tire design and type (pneumatic, solid, low-pressure, etc.), internal inflation pressure, wheel load, tire stiffness, as well as the physical and mechanical properties of the soil and its moisture conditions.

Excessive vertical stress may lead to degradation of soil structure, reduction in porosity, and decreased water permeability, which negatively affects plant growth conditions and crop yield. Therefore, during the design and operation of machine–tractor units, it is important to ensure an optimal ground pressure that does not exceed the allowable soil bearing capacity.

Both experimental methods (e.g., measurements using strain gauge sensors) and mathematical models are used to evaluate vertical stress. Analytical models take into account tire parameters and soil characteristics and allow predicting the influence of changes in load, tire inflation pressure, or travel speed on the magnitude and distribution of stress.

Before proceeding to the determination of vertical stress distribution beneath the center of a wheel, it is necessary to define the contact patch area, which is characterized by its length ak and width bk (Figure 1). The determination of ak and bk can be based on well-established semi-empirical models [7, 9], including the Lyasko model [10], the Schwanghart model [8], and the Saarilahti model [11]. Among these, the Lyasko model [10] has gained significant popularity, as it determines the contact patch dimensions while accounting for the radial deformation of the tire:

$$a_k = \frac{23}{11,9 + \left|\frac{D}{b} - 3,5\right|}\sqrt{D \cdot f_t - f_t^2}\,; \qquad (1)$$

$$b_k = 2\sqrt{\frac{\left(b + 0,5\left(D - 0,0254 \cdot D_p\right)\right)}{2,5} \cdot f_t - f_t^2}\,, \qquad (2)$$

where D is tire outer diameter; b is tire profile width; f_t is radial deformation of the tire; D_p is nominal rim mounting diameter in inches.

Note that in [12], it is proposed to modify equation (1) by incorporating the tire ply rating index n_c

$$a_k = \frac{23}{11,9 + \left|\frac{D}{b} - \frac{|n_c - 9|}{2} - 3,5\right|}\sqrt{D \cdot f_t - f_t^2}\,. \qquad (3)$$

The author of [12] claims that taking into account the value of n_c will allow to approximate the value of the calculated area of the tire contact patch to the value of the nominal contour area of the patch, which is obtained from test data or manufacturer's estimated calculations. However, this approach requires experimental confirmation.

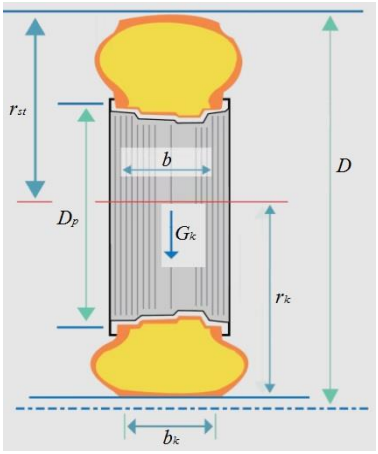

Figure 1: Tire components under vertical load

The next step in the Lyasko model [10], as well as in [12], assumes that the tire–soil contact patch area has an elliptical shape:

$$F_k = \frac{\pi \cdot a_k \cdot b_k}{4}. \tag{4}$$

Equation (6) is not entirely accurate. As demonstrated in studies [7, 5, 13], the contact patch of an agricultural tire should be described by a superellipse shape. The contact area in the form of a superellipse has been presented in [5, 13], and its equation in an orthogonal coordinate system can be expressed as follows:

$$\left|\frac{x}{0.5 \cdot a_k}\right|^n + \left|\frac{y}{0.5 \cdot b_k}\right|^n \le 1, \tag{5}$$

where x and y are the superellipse coordinates; n is the superellipse exponent.

In an orthogonal coordinate system, the superellipse exponent n is a positive real number that defines the shape of the superellipse, while the parameters $0.5 \cdot a_k$ and $0.5 \cdot b_k$ are the semiaxes that define its size. Varying the value of the exponent n allows for a wide range of curves [14]. The curve for $n = 2$ is an ellipse (for $0.5 \cdot a_k = 0.5 \cdot b_k$ it is a circle). As n decreases to 1, the curve forms a peak at the vertex; the curve for $n = 1$ is a parallelogram (rhombus). For $n > 2$, the sides of the curve flatten out, and the shape of the curve begins to resemble a rectangle (Figure 2).

Considering equation (7), the contact patch area is determined using the following expression [13]:

$$F_k = a_k \cdot b_k \cdot \frac{G_f\left(1+\frac{1}{n}\right)^2}{G_f\left(1+\frac{2}{n}\right)} \text{ or } F_k = b_k \cdot \int_0^{a_k}\left(1-\left(\frac{x}{a_k}\right)^n\right)^{1/n} dx, \tag{6}$$

where G_f is the gamma function.

From study [7], experimental investigations confirmed that the exponent n, which is an essential parameter for determining the area of a superellipse, should be equal to 3.2. Accordingly, equation (6) takes the following form:

$$F_k \approx 0.9 \cdot a_k \cdot b_k. \tag{7}$$

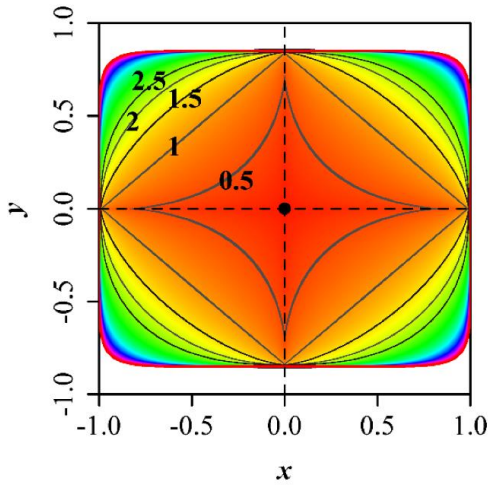

Figure 2: The shape of a superellipse depending on the exponent n and the value of the half-length [15]

For the correct determination of the contact patch area, it is also necessary to establish the value of the radial tire deformation, which according to the Lyasko model [10] is expressed as follows:

$$f_t = \frac{c_2 \cdot G_k}{2\left(p_t + p_0\right)} + \sqrt{\left(\frac{c_2 \cdot G_k}{2\left(p_t + p_0\right)}\right)^2 + c_1 \cdot G_k}, \tag{8}$$

where c_1, c_2 are the constant coefficients determined based on the Biederman model, which is highlighted in [12]; G_k is the tire load; p_0 is the constant coefficient of pressure characteristic depending on carcass stiffness for zero internal pressure conditions [12].

$$p_0 = \left(16,7 \cdot \left(n_c - 1\right) \cdot \sqrt{\frac{D}{b} - 1,4}\right) - 28. \tag{9}$$

Also, for calculations, it is necessary to take into account the value of the dynamic radius of the tire, which is determined by the classical equation:

$$r_k = 0,5D - f_t. \tag{10}$$

After calculating all components, the determination of the vertical stress distribution under the center of the wheel can be calculated using the Becker formula [3]:

$$\sigma_z\left(z\right) = P_0 \cdot \left(1 - \frac{z^3}{\left(z^2 + r_0^2\right)^{3/2}}\right), \tag{11}$$

where P_0 is the pressure at the contact point between the tire and the ground; z is the depth at which vertical stress acts; r_0 is the radius of the load area.

The use of equation (11) involves certain limitations and inaccuracies, as it is derived under the assumption that the tire contact patch has a circular shape. For a contact patch in the form of a superellipse (equation (7)), it is necessary to determine an equivalent circular area with radius r_0:

$$r_0 = \sqrt{\frac{0.9 \cdot a_k \cdot b_k}{\pi}} \approx 0.54 \cdot \sqrt{a_k \cdot b_k} \,. \tag{12}$$

Then, taking into account equation (12), we change (11):

$$\sigma_z(z) = P_0 \cdot \left(1 - \frac{z^3}{\left(z^2 + 0.29 \cdot a_k \cdot b_k \right)^{3/2}} \right). \tag{13}$$

Thus, a complete mathematical algorithm for determining the vertical stress distribution on the soil is presented.

3.2. Selection and Technical Characteristics of Tractor Tires for the Case IH Magnum 400

Selection and Technical Characteristics of Tractor Tires for the Case IH Magnum 400

Currently, on the Ukrainian market, the Case IH Magnum 400 tractor can be equipped with tires from various manufacturers. In this study, attention is focused on options representing the mid-range segment, namely the Trelleborg [16] and Mitas [17] brands (Figure 3).

Trelleborg [16] is one of the leading manufacturers of tires for agricultural machinery, particularly for high-power tractors. The company is currently part of the Yokohama Rubber Company. Its product portfolio includes tire series designed to enhance traction performance and improve tire–soil interaction efficiency.

In particular, the TM Progressive Traction® series (TM900, TM1000, TM700) is characterized by a tread design featuring dual lugs, which contribute to improved traction, self-cleaning capability, and a more uniform load distribution. The TM1000 model is intended for use with high-performance tractor units. Special attention is also given to the TM1 ECO POWER model, introduced at Agritechnica 2023, which incorporates design solutions aimed at reducing rolling resistance and increasing the share of renewable materials in its composition.

a b

Figure 3: Tested rear tires Trelleborg 710/75 R42(a) and Mitas 710/70 R42(b)

Mitas [17] is a European tire manufacturer that is part of the Trelleborg Group and specializes in products for agricultural, industrial, and other types of machinery. The company implements IF (Increased Flexion) and VF (Very High Flexion) technologies, which enable tire operation at reduced inflation pressure while maintaining the permissible load capacity. This contributes to reduced soil compaction and improved traction performance of tractor–implement units. The company's products are widely used on tractors of medium and high power classes.

The technical specifications of Trelleborg and Mitas tires used on the Case IH Magnum 400 tractor are presented in Table 1.

The minimum and maximum permissible tire loads presented in Table 1 require clarification. As noted in studies [12, 20], when operating under traction conditions, the allowable tire loads should be determined based on the speed symbol A6 (i.e., 30 km·h^{-1}). This necessitates recalculation of the load values by increasing the tabulated data by 15%.

Table 1: Technical characteristics of the tires

Brand	Standard size	D, m	b, m	r_c, m	$\bar{G}_{k\max}$, kg	$p_{t.\max}$, kPa	$\bar{G}_{k\min}$, kg	$p_{t.\min}$, kPa	Index
Trelleborg [18]	600/70 R30	1.608	0.605	0.722	5730	240	2695	60	158D
	710/75 R42	2.14	0.72	0.945	9750	240	4235	60	175D
Mitas [19]	600/70 R30	1.595	0.625	0.7	4970	160	3295	60	152D
	710/70 R42	2.07	0.731	0.935	9100	240	4970	60	173D

4. Results

As a next step, the dependence of the tire contact patch area is constructed based on equations (1), (2), and (7) as a function of permissible loads and tire inflation pressure. The results are presented in Figures 4 and 5.

Analyzing the results presented in Figures 4 and 5, it can be observed that the contact patch area of Trelleborg and Mitas tires varies over a wide range:

1. Trelleborg:

- 600/70 R30: at inflation pressure $p_{t1} \in [60; 240]$ kPa, the contact patch area $F_{k1} \in [0.251; 0.1]$ m²;
- 710/75 R42: at inflation pressure $p_{t2} \in [60; 240]$ kPa, the contact patch area $F_{k2} \in [0.458; 0.131]$ m²;

2. Mitas:

- 600/70 R30: at inflation pressure $p_{t1} \in [60; 160]$ kPa, the contact patch area $F_{k1} \in [0.273; 0.21]$ m²;
- 710/70 R42: at inflation pressure $p_{t2} \in [60; 240]$ kPa, the contact patch area $F_{k2} \in [0.396; 0.235]$ m².

It should be noted that boundary "A" indicates conditions under which tire operation is not recommended, whereas boundary "B" corresponds to acceptable operating conditions. Based on this, the ranges of variation of the tire contact patch areas can be identified as follows: for the Trelleborg 600/70 R30 tire, at an inflation pressure $p_{t1} \in [170; 240]$ kPa, the contact area $F_{k1} \in [0.251; 0.194]$ m²; for the Trelleborg 710/75 R42 tire, at $p_{t2} \in [180; 240]$ kPa, the contact area $F_{k2} \in [0.462; 0.365]$ m²; for the Mitas 600/70 R30 tire, at $p_{t1} \in [130; 160]$ kPa, the contact area $F_{k1} \in [0.272; 0.257]$ m²; and for the Mitas 710/70 R42 tire, at $p_{t2} \in [185; 240]$ kPa, the contact area $F_{k2} \in [0.396; 0.35]$ m².

Evaluating the obtained relationships, it should be noted that when comparing the values at minimum and maximum tire inflation pressure over the entire range of permissible loads (as specified by the manufacturer), the Mitas 600/70 R30 tire provides a contact patch area that is 8–52.3% larger than that of the Trelleborg 600/70 R30 tire. A similar trend is observed for the rear tires: the Trelleborg 710/75 R42 tire exhibits a 13.5% larger contact area compared to the Mitas 710/70 R42 tire at minimum inflation pressure, whereas at maximum pressure the Mitas 710/70 R42 tire provides a 44.3% larger contact area compared to the Trelleborg 710/75 R42 tire.

The obtained results reveal certain inconsistencies, since the range of loads specified by the manufacturer may significantly differ from the actual loads acting during the operation of a specific Case IH Magnum 400 tractor. Therefore, the values obtained in Figures 4 and 5 require further refinement through experimental validation, for example, based on test cycles conducted by the Nebraska Tractor Test Laboratory.

The next step is to identify the loads acting on the tractor axles in order to determine the minimum and maximum permissible ranges of load variation and tire inflation pressure. According to [21], the total operating weight of the wheeled Case IH Magnum 400 tractor, including the operator, is m = 14292 kg, with 5216 kg distributed on the front axle and 9076 kg on the rear axle. Taking this into account, these data were incorporated into Figures 4 and 5, and the corresponding results for Trelleborg and Mitas tires are presented in Figures 6 and 7.

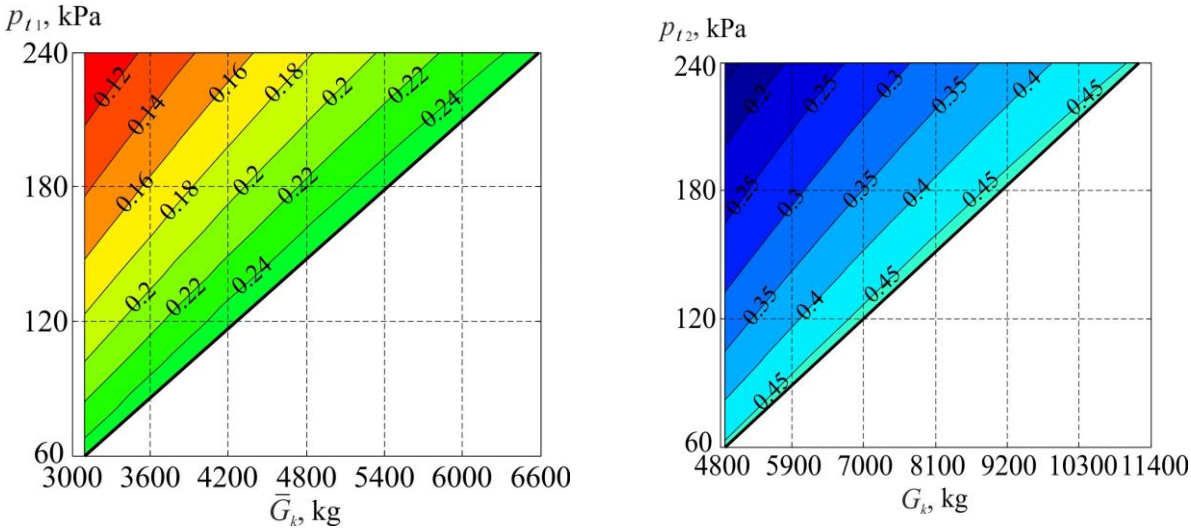

a b

Figure 4: Change in the contact patch area F_k (m²) of Trelleborg tires (F_k, m²) depending on tire pressure p_t (kPa) and permissible loads $\bar{G}_k$ (kg) at front tire 600/70 R30 (a) and rear tire 710/75 R42(b)

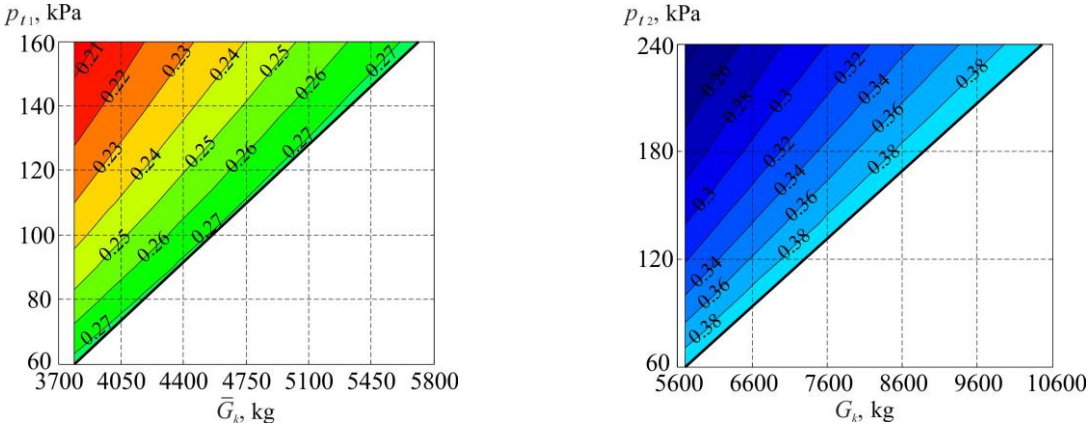

a b

Figure 5: Change in the contact patch area F_k (m^2) of Mitas tires (F_k, m^2) depending on tire pressure p_t (kPa) and permissible loads $\bar{G}_k$ (kg) at front tire 600/70 R30 (a) and rear tire 710/70 R42(b)

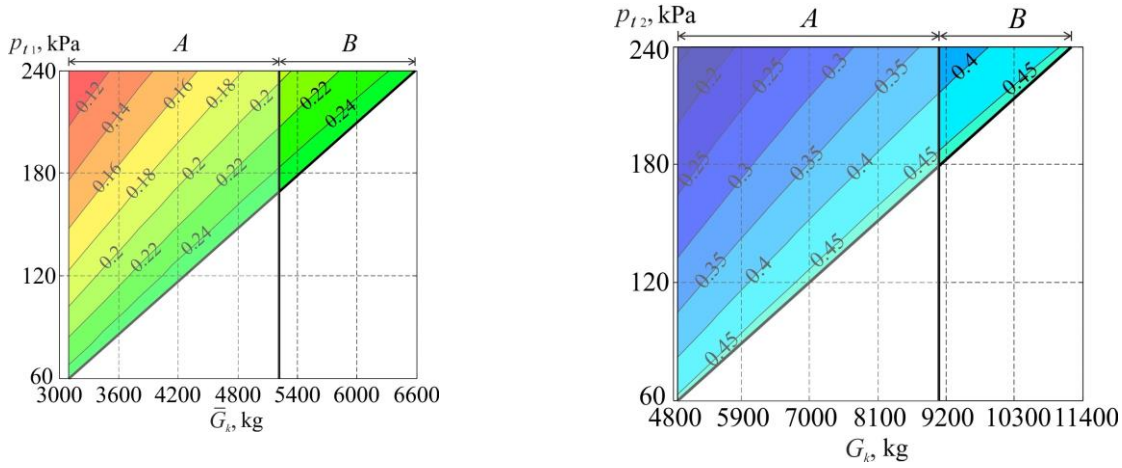

a b

Figure 6: Change in the contact patch area F_k (m^2) of Trelleborg tires (F_k, m^2) depending on tire pressure p_t (kPa) and permissible loads $\bar{G}_k$ (kg) taking into account the load on front tire 600/70 R30(a) and rear tire 710/75 R42(b)

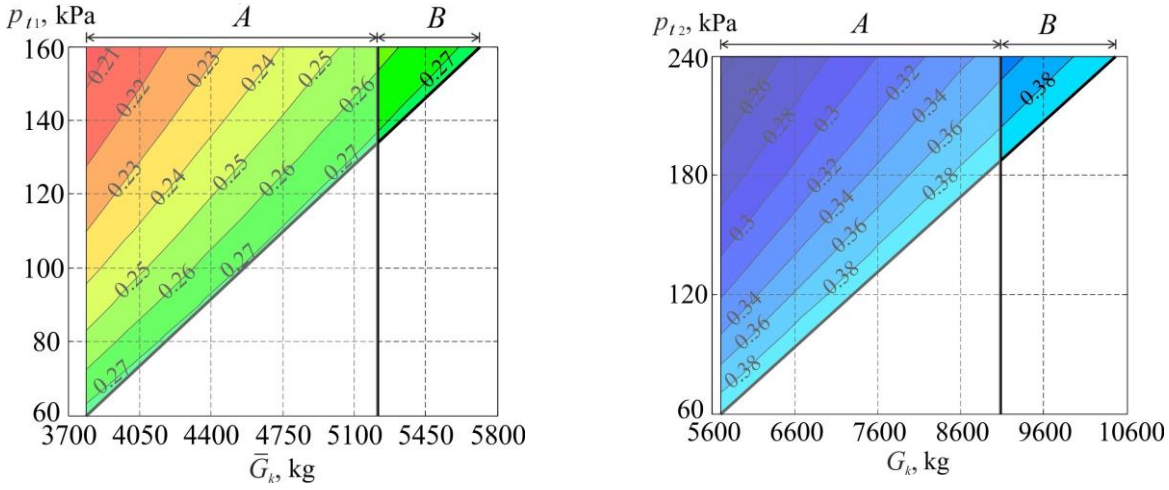

a b

Figure 7: Change in the contact patch area F_k (m^2) of Mitas tires (F_k, m^2) depending on tire pressure p_t (kPa) and permissible loads $\bar{G}_k$ (kg) taking into account the load on front tire (600/70 R30(a) and rear tire 710/70 R42(b)

5. Discussion

The obtained results are generally consistent with previously reported experimental and analytical studies, confirming that the contact area increases with vertical load and decreases with inflation pressure, although this relationship is not strictly linear. Earlier findings showed that doubling the load leads to only a 30–40% increase in contact area, while doubling inflation pressure reduces it to approximately 70–80% of its initial value [8], which aligns well with the trends observed in the present modeling.

A good agreement is also observed with studies demonstrating that geometrical approaches, particularly those based on superellipse approximation, provide high accuracy in predicting the tire–soil contact area, reaching up to 81–95% agreement with experimental data [7]. This supports the applicability of geometry-based modeling approaches used in this study. Similarly, recent experimental work confirmed that reducing inflation pressure significantly increases the contact length, especially under higher loads, while also showing that the contact area on deformable soil can be several times larger than on rigid surfaces [9]. This highlights the importance of accounting for soil deformation in modeling.

At the same time, other studies reveal more complex behavior of tire–soil interaction. In particular, it has been shown that under low load conditions, reducing inflation pressure does not necessarily increase the contact area; in some cases, the opposite effect may occur due to increased tire curvature and elastic deformation [6]. This indicates that the commonly assumed inverse relationship between pressure and contact area is mainly valid for higher load levels. Furthermore, tire structure, dimensions, and type were identified as statistically significant factors, while the relationship between soil hardness and contact area was found to be non-linear [22].

These findings are further supported by subsequent research, where it was demonstrated that reliable prediction of contact area requires not only load and inflation pressure but also intrinsic tire properties such as stiffness and specific contact area [23]. It was also shown that the influence of inflation pressure becomes less pronounced for larger tires unless additional parameters are included, and that classification of tires into size-based groups improves prediction accuracy [23]. In contrast, the current model focuses primarily on external parameters, which allows capturing the dominant trends but limits its applicability under varying soil and tire conditions.

Overall, the comparison confirms that the proposed modeling approach adequately reproduces the main trends reported in the literature, while also indicating that tire–soil interaction is governed by a combination of geometric, mechanical, and soil-related factors. The results emphasize that simplified monotonic assumptions regarding the relationship between inflation pressure and contact area may not be sufficient for accurately describing real operating conditions, particularly across different tire types and load regimes.

6. Conclusions

The conducted study confirmed that inflation pressure and permissible load are the main factors affecting the contact patch area of agricultural tires. An increase in vertical load leads to an increase in the contact area, whereas higher inflation pressure generally reduces it. The obtained dependencies are nonlinear and vary depending on operating conditions.

A mathematical approach for calculating the tire–soil contact patch area was systematized. The proposed method combines the classical Lyasko model for determining contact length and width with a superellipse-based representation of the contact geometry [14], which provides a more accurate description of the actual tire–soil interaction conditions.

The operating parameters and technical characteristics of Trelleborg and Mitas tires used on the Case IH Magnum 400 tractor were identified and analyzed. For the Trelleborg 600/70 R30 tire, at an inflation pressure range of 170–240 kPa, the contact area varied from 0.251 to 0.194 m^2. For the Trelleborg 710/75 R42 tire, at 180–240 kPa, the contact area ranged from 0.462 to 0.365 m^2.

For the Mitas 600/70 R30 tire, at an inflation pressure range of 130–160 kPa, the contact area varied from 0.272 to 0.257 m^2. For the Mitas 710/70 R42 tire, at 185–240 kPa, the contact area ranged from 0.396 to 0.350 m^2.

Comparative analysis showed that the Mitas 600/70 R30 tire provides an 8–52.3% larger contact patch area than the Trelleborg 600/70 R30 tire within the investigated operating range. For rear tires, the Trelleborg 710/75 R42 tire exhibited a 13.5% larger contact area at minimum inflation pressure, whereas at maximum pressure the Mitas 710/70 R42 tire provided a 44.3% larger contact area.

The proposed model can be applied for engineering estimation of tire operating regimes and for evaluating the influence of inflation pressure and permissible loads on contact patch geometry under agricultural operating conditions.

Acknowledgements

The study was conducted within the framework of the implementation of the state budget research topic No 0126U000479 "Increasing soil fertility by reducing the impact of external mechanical and chemical factors during the cultivation of agricultural crops", approved by order of the

Ministry of Education and Science No. 22 and No. 23 of January 9, 2026.

References

[1] Roşca, R., Cârlescu, P., Ţenu, I., Vlahidis, V., & Perşu, C. (2022). The improvement of a traction model for agricultural tire–soil interaction. *Agriculture*, 12(12), 2035. https://doi.org/10.3390/agriculture12122035

[2] Lebedev, A., Shuliak, M., Lebedev, S., Khalin, S., Haidai, T., et al. (2024). Determining conditions for providing maximum traction efficiency of tractor as part of a soil tillage unit. *Eastern-European Journal of Enterprise Technologies*. 1(1 (127), 6 – 14. https://doi.org/10.15587/1729-4061.2024.297902

[3] Lebedev, A., Shuliak, M., Khalin, S., Lebedev, S., Szwedziak, K., et al. (2023). Methodology for assessing tractor traction properties with instability of coupling weight. *Agriculture*, 13(5), 977. https://doi.org/10.3390/agriculture13050977

[4] Kukharets, S., Zabrodskyi, A., Sheludchenko, B. et al. (2025). Assessment of changes in soil contact stress depending on tractor tire parameters. *Sci Rep* 15, 172. https://doi.org/10.1038/s41598-024-84102-y

[5] Wong, J.Y. (2010). Terramechanics and off-road vehicle engineering (second edition) *Oxford. Elsevier*, UK. https://doi.org/10.1016/C2009-0-00403-6

[6] Ptak, W., Czarnecki, J., Brennensthul, M., Lejman, K., & Małecka, A. (2023). Evaluation of tires acting on soil in field conditions using the 3D scanning method. *Agriculture*, *13*(5), 1094. https://doi.org/10.3390/agriculture13051094

[7] Marušiak M, Zemánek T, Neruda J, Nevrkla P. (2024). Calculation and operational assessment of tyre contact areas in the tractor-and-trailer unit. *J. For. Sci.*, 70(3), 144 – 159. doi: 10.17221/109/2023-JFS

[8] Schwanghart H. (1991). Measurement of contact area, contact pressure and compaction under tyres in soft soil. *Proceedings of the 10th ISTVS Conference*. Volume 1. Kobe, Aug 20-24, 1990, 193 – 204. https://doi.org/10.1016/0022-4898(91)90012-U

[9] Alkhalifa N., Tekeste M.Z., Jjagwe P., Way T.R. (2024). Effects of vertical load and inflation pressure on tire-soil interaction on artificial soil, *Journal of Terramechanics,* 112, 19 – 34, https://doi.org/10.1016/j.jterra.2023.11.002

[10] Lyasko M.I. (1994). The determination of deflection and contact characteristics of a pneumatic tyre on a rigid surface. *Journal of Terramechanics,* 31, 239 – 242. https://doi.org/10.1016/0022-4898(94)90019-1

[11] Saarilahti, M. (2002). Soil interaction model. University of Helsinki, Department of Forest Resource Management. – available at: https://helda.helsinki.fi/server/api/core/bitstreams/f76aeb7a-bf28-4143-ae1e-b0bfaaa62ba3/content

[12] Kozhushko A.; Rebrov, O.; Kalchenko, B.; Sirovitskiy, K.; Mudryi, Y. (2024). Analysis of the Efficiency of Agricultural Tires for Low-Power Electric Tractors. *4th International Conference on Reliable Systems Engineering*, ICoRSE 2024. Lecture Notes in Networks and SystemsVolume 1129 LNNS, 61 – 70. doi: https://doi.org/10.1007/978-3-031-70670-7_5

[13] Keller, T. (2005). A model for the prediction of the contact area and the distribution of vertical stress below agricultural tyres from readily available tyre parameters. *Biosystems Engineering,* 92(1), 85 – 96. https://doi.org/10.1016/j.biosystemseng.2005.05.012

[14] Spíchal, L. (2020). Superelipsa a superformule (Superellipse and superformula). *Matematika-Fyzika-Informatika*, 29(1), 54 – 69. https://mfi.upol.cz/files/29/2901/mfi_2901_054_069.pdf

[15] Huang, W., Li, Y., Niklas, K. J., Gielis, J., Ding, Y., Cao, L., & Shi, P. (2020). A Superellipse with Deformation and Its Application in Describing the Cross-Sectional Shapes of a Square Bamboo. *Symmetry*, 12(12), 2073. https://doi.org/10.3390/sym12122073

[16] Trelleborg. (n.d.). TM900 ProgressiveTraction: Superior grip for high-power tractors. – available at: TM900 ProgressiveTraction® page

[17] Mitas Tires. (n.d.). SFT – Tractor radial tyres. – available at: SFT product page

[18] Trelleborg. (n.d.). Technical manual. – available at: https://www.trelleborg-tires.com/-/media/tires-aft/datatsheet/technical-manual/trelleborg-technical-manual-en.pdf

[19] Mitas Tires. (2023). Agricultural tires: Technical manual. – available at: https://www.mitas-tires.com/-/media/mitas-tyres/catalogues-leaflets/mitas_agri_2023_en_lr.pdf?rev=-1

[20] Anifantis, A.S.; Cutini, M.; Bietresato, M. (2020). An Experimental–Numerical Approach for Modelling the Mechanical Behaviour of a Pneumatic Tyre for Agricultural Machines. *Appl. Sci*., 10, 3481. https://doi.org/10.3390/app10103481

[21] Nebraska Tractor Test Lab. (2022). Test 2242: Case IH Magnum 400. University of Nebraska–Lincoln. – available at: https://digitalcommons.unl.edu/cgi/viewcontent.cgi?article=4376&context=tractormuseumlit

[22] Diserens, E. (2009). Calculating the contact area of trailer tyres in the field. *Soil and Tillage Research*, 103(2), 302 – 309. https://doi.org/10.1016/j.still.2008.10.020

[23] Diserens, E., Défossez, P., Duboisset, A., & Alaoui, A. (2011). Prediction of the contact area of agricultural traction tyres on firm soil. *Biosystems Engineering*, 110(2), 73 – 82. https://doi.org/10.1016/j.biosystemseng.2011.06.008